CATALYTIC ACTIVITY STUDY OF Ni_xSn_y INTERMETALLICS

Anchernsiri Noomnual

A Thesis Submitted in Partial Fulfillment of the Requirements
for the Degree of Master of Science
The Petroleum and Petrochemical College, Chulalongkorn University
in Academic Partnership with
The University of Michigan, The University of Oklahoma,
and Case Western Reserve University
2017

Thesis Title: Catalytic Activity Study of Ni_xSn_y Intermetallics
By: Anchernsiri Noomnual
Program: Polymer Science
Thesis Advisors: Prof. Sujitra Wongkasemjit
Assoc. Prof. Thanyalak Chaisuwan

Accepted by The Petroleum and Petrochemical College, Chulalongkorn University, in partial fulfillment of the requirements for the Degree of Master of Science.

………………………………….. College Dean
(Prof. Suwabun Chirachanchai)

Thesis Committee:

....
(Prof. Sujitra Wongkasemjit)

....
(Assoc. Prof. Thanyalak Chaisuwan)

....
(Prof. Apanee Luengnaruemitchai)

....
(Dr. Ruangdaj Tongsri)

ABSTRACT

5872001063: Polymer Science Program
Anchernsiri Noomnual: Catalytic Activity Study of Ni_xSn_y Intermetallics.
Thesis Advisors: Prof. Sujitra Wongkasemjit, and Assoc. Prof. Thanyalak Chaisuwan 40 pp.

Keywords: Nickel-tin intermetallics/ Chemical reaction

Cinnamyl alcohol (COL), versatile chemical in fragrance, flavoring, and pharmaceutical industries, can be found in only small amounts in nature. Generally, COL can be synthesized via selective hydrogenation of cinnamaldehyde (CALD), natural oil, at aldehyde functional group under high pressure of hydrogen gas. In this work, Ni_xSn_y intermetallics were used as catalysts in selective hydrogenation to obtain COL. These catalysts were synthesized via mechanical alloying, economic and environmental method, and characterized by X-ray diffraction (XRD). By using 43, 58, and 75% tin contents with nickel, Ni_3Sn, Ni_3Sn_2, and Ni_3Sn_4 intermetallics were prepared, respectively. In addition, formic acid was used as a proton-hydride source to convert CALD to COL. The optimal time, temperature, type and amount of Ni_xSn_y catalyst, and also rate of formic acid adding were studied. The result showed that the optimal conditions were 300 mg Ni_3Sn_4, 5 mmol CALD and 25 µl per 5 min of FA in 10 ml THF at 60 °C for 3 h reaction time to the maximum yield of COL. Under these conditions, COL was obtained at 1.8% yield with 36.7% conversion. However, other products (hydrocinnamyl alcohol, hydrocinnamaldehyde, cinnamic acid, and benzaldehyde) were also detected by gas chromatography-flame ionization detector (GC-FID).

บทคัดย่อ

อัญเชิญสิริ นุ่มนวล : การศึกษาความสามารถในการเป็นตัวเร่งปฏิกิริยาของสารประกอบนิกเกิล-ดีบุก (Catalytic Activity Study of Ni_xSn_y Intermetallics) อ.ที่ปรึกษา: ศ.ดร. สุจิตรา วงศ์เกษมจิตต์ และ รศ.ดร.ธัญลักษณ์ ฉายสุวรรณ์ 40 หน้า

ซินนามิลแอลกอฮอล์เป็นสารเคมีที่ใช้ประโยชน์ได้หลากหลาย ทั้งในอุตสาหกรรมยา การแต่งกลิ่นและรสชาติ แต่หนึ่งในข้อจำกัดของซินนามิลแอลกอฮอล์คือ พบได้ในปริมาณน้อยในธรรมชาติ ดังนั้น โดยส่วนมากซินนามิลแอลกอฮอล์ที่นำมาใช้จึงได้มาจากการสังเคราะห์โดยกระบวนการเติมไฮโดรเจนที่ตำแหน่งคาร์บอนิลของซินนามาลดีไฮด์ การสังเคราะห์ซินนามิลแอลกอฮอล์ผ่านกระบวนการดังกล่าวโดยทั่วไปนั้นมักทำภายใต้สภาวะความดันสูงทำให้ส่งผลต่อทั้งความปลอดภัยและต้นทุนในการผลิต ในงานวิจัยนี้จึงมุ่งเน้นที่จะสังเคราะห์ซินนามิลแอลกอฮอล์โดยใช้สารประกอบโลหะนิกเกิล-ทินเป็นตัวเร่งปฏิกิริยา สารประกอบโลหะนิกเกิล-ทินในงานวิจัยนี้สังเคราะห์ได้จากกระบวนการบดผสมแบบเชิงกลและให้ความร้อนซึ่งเป็นวิธีที่มีต้นทุนต่ำและเป็นมิตรกับสิ่งแวดล้อม และใช้เทคนิค XRD ในการวิเคราะห์สารประกอบโลหะดังกล่าว จากการใช้สัดส่วนที่แตกต่างกันของนิกเกิลและทิน ได้แก่ 43, 58 และ 75% ของทินทำให้ได้เกิดสารประกอบโลหะที่แตกต่างกันคือ Ni_3Sn, Ni_3Sn_2 และ Ni_3Sn_4 ตามลำดับ นอกจากนี้ กรดฟอร์มิกยังถูกใช้เป็นสารตั้งต้นร่วมกับซินนามาลดีไฮด์เพื่อทำหน้าที่ผลิตไฮไดรด์ให้กับระบบ ในแง่ของการทำปฏิกิริยาสภาวะที่เหมาะสมสำหรับปฏิกิริยาย่อมมีส่วนสำคัญต่อการดำเนินไปของปฏิกิริยา ดังนั้น ในงานวิจัยนี้จึงศึกษาอุณหภูมิ, เวลา, ชนิดและปริมาณของตัวเร่งปฏิกิริยา รวมทั้งปริมาณของกรดฟอร์มิกที่เหมาะสมเพื่อให้ได้ซินนามิลแอลกอฮอล์ปริมาณมากที่สุด จากผลการทดลองพบว่าสภาวะที่ทำให้ได้ซินนามิลแอลกอฮอล์มากที่สุดคือ เมื่อใช้เตตระไฮโดรฟูแรน 10 ml เป็นสารละลาย และ ใช้ Ni_3Sn_4 300 mg เป็นตัวเร่งปฏิกิริยาที่อุณหภูมิ 60 องศาเซลเซียส เวลา 3 ชั่วโมง ให้ผลของปฏิกิริยามากที่สุดเท่ากับร้อยละ 36.65 และผลิตภัณฑ์ซินนามิลแอลกอฮอล์ร้อยละ 1.83 ภายใต้การกลั่นแบบรีฟลักซ์ อย่างไรก็ตามปฏิกิริยาที่เกิดขึ้นสามารถเกิดผลิตภัณฑ์อื่นๆด้วย ได้แก่ ไฮโดรซินนามาลดีไฮด์, ไฮโดรซินนิมิลแอลกอฮอล์, กรดซินนามิก และ เบนซัลดีไฮด์ ซึ่งผลิตภัณฑ์ที่เกิดขึ้นวิเคราะห์โดยใช้เทคนิค GC-FID

ACKNOWLEDGEMENTS

First of all, I would like to express my sincere gratitude to my advisor, Prof. Sujitra Wongkasemjit, for her kindness and encouragement. She always motivates, advices, and guides me not only in academic way but also in the way of living. I also would like to thank my co-advisor, Assoc. Prof. Thanyalak Chaisuwan, for her support and great suggestions.

Besides my advisor and co-advisor, I would like to express my deepest appreciation to my committees, Prof. Apanee Luengnaruemitchai and Dr. Ruangdaj Tongsri, for their insightful comments with widen and various perspectives to accomplish my thesis.

I also would like to express my special thanks to Mr. Sakollapath Pithakratanayothin who always suggests, supports, and cheers me up. Furthermore, I would like to extend my thankfulness to SW & TC group members for their help and cheerfulness. We have a lot of meaningful experiences and good memories together.

I would like to take this opportunity to thank all members and staffs of the Petroleum and Petrochemical College, Chulalongkorn University.

I am grateful for the full scholarship and full funding of the thesis work provided by the Petroleum and Petrochemical College.

This thesis work is funded by the Petroleum and Petrochemical College and Center of Excellence on Petrochemical and Materials Technology.

This research work was also supported by a grant from the Grant for International Research Integration: Chula Research Scholar, Ratchadaphiseksompote Endowment Fund, Chulalongkorn University, Thailand.

Last but not least, I must express my very profound gratitude to my parents and my sister for their supports, love and standing by me all the time.

Anchernsiri Noomnual
29 April 2017

TABLE OF CONTENTS

LIST OF TABLES

TABLE **PAGE**

LIST OF FIGURES

FIGURE **PAGE**

FIGURE **PAGE**

ABBREVIATIONS

2-Me-THF	2-metyl-tetrahydrofuran
CALD	Cinnamaldehyde
CO	Carbonmonoxide
CO_2	Carbondioxide
COL	Cinnamyl alcohol
e^-	Electron
equiv.	Equivalent
EtOH	Ethanol
GC-FID	Gas chromatography-flame ionization detector
H^+	Proton
H_2O	Water
HCALD	Hydrocinnamaldehyde
HCOL	Hydrocinnamyl alcohol
im-	Impregnated
i-PrOH	*iso*-Propanol
MA	Mechanical alloying
MAed	Mechanical alloyed
MeOH	Methanol
t-AmOH	*tert*-Amyl alcohol
THF	Tetrahydrofuran
XRD	X-rays diffraction spectroscopy

LIST OF SYMBOLS

α	Alpha
β	Beta
C=C	Carbon carbon double bond
C=O	Carbon oxygen bond
˚C	Degree celsius
ΔG	Gibb's free energy
h	Hour
μL	Microliter
mg	Milligram
mL	Milliliter
mmol	Millimole
min	Minute
Ni_xSn_y	Nickel tin intermetallic
ɳ	Nu
Pd	Palladium
π	Pi
Pt	Platinum
rpm	Revolutions per minute
Ru	Rubidium
σ	Sigma
Sn	Tin.

CHAPTER I

INTRODUCTION

Cinnamyl alcohol (COL) is used in perfume, cosmetics, pharmaceutical, and chemical industry. The precursor of COL is cinnamaldehyde (CALD) which is a type of α,β-unsaturated aldehyde. CALD can be hydrogenated to hydrocinnamaldehyde (HCALD) or cinnamyl alcohol (COL), depending on the hydrogenated position (Gallezot *et al.*, 1998; Chen *et al.*, 2012; Gutiérrez *et al.*, 2013; Lin *et al.*, 2013; Durndell *et al.*, 2015).

In this work, our hydrogen source is formic acid (FA) due to its high hydrogen content (Yadav *et al.*, 2012), nontoxicity, being liquid at room temperature, and recharging ability, meaning that FA is decomposed to carbon dioxide (CO_2) and hydrogen (H_2), and obtained by hydrogen reduction with CO_2 (Singh *et al.*, 2016). Generally, there are 2 pathways of formic acid decomposition, dehydrogenation and dehydration, as shown in Figure 1.1. Generation of H_2 and CO_2 via dehydrogenation is the desirable pathway since the dehydration pathway provides carbon monoxide (CO) which is rather toxic (Yoo *et al.*, 2014).

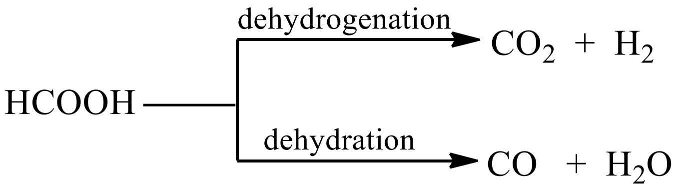

Figure 1.1 Pathways of formic acid decomposition.

When CO generating via dehydration is adsorbed on metal catalyst surface, the number of active sites and activity of the catalyst decrease. However, the adsorbed CO is oxidized on metal surface by hydroxide from water dissociation and converted to CO_2 before leaving the metal surface.

After CO_2 removal, the surface is once again free for dehydrogenation to produce CO_2 and H_2 (Stevanović *et al.*, 2014). Therefore, the catalysts indeed play an important role not only in selective hydrogenation of α, β-unsaturated aldehyde, but also achieving high quantity of H_2 and CO_2 from decomposition of formic acid and diminishing CO adsorption on metal catalyst surface.

Typically, monometallic catalysts, such as platinum (Pt) and palladium (Pd), are widely applied in hydrogenation reactions, but because of its high value, nickel (Ni), which is also a Pt-group metal, is, thus, a good candidate due to its similar catalytic behavior to Pt (Gallezot *et al.*, 1998). Moreover, FA could be decomposed on Ni surface as well as on Pt or Pd surface to generate H_2 and CO_2 (Luo *et al.*, 2012; Luo *et al.*, 2013). Unfortunately, the α, β-unsaturated aldehyde hydrogenation of the C=C bond is comparatively easier than that of the C=O bond and the decomposition of formic acid to water and carbon monoxide easily occurs by using monometallic catalysts, for example, copper (Cu) (Gutiérrez *et al.*, 2013), Pt (Guo *et al.*, 2014), Ag (Mertens *et al.*, 2007; Mertens *et al.*, 2009), Au (Mertens *et al.*, 2009). Thus, addition of a second metal, e.g. Ir (Lin *et al.*, 2013), Co (Malobela *et al.*, 2014), Au (Prakash *et al.*, 2016), and Sn (Taniya *et al.*, 2012; Rautio *et al.*, 2015) to form intermetallic or alloy catalysts could lead to an increasing tendency of hydrogenation at the C=O bond since charge transfer occurs from the second metal atom to the first metal atom, resulting in increasing electron density around the first metal, causing repulsive force between four electrons at the C=C bond and metal surface. Moreover, the presence of electropositivity of the second metal atom induces the polarization at the C=O bond, leading to more hydrogenation at the C=C position (Li *et al.*, 2013; Lin *et al.*, 2013; Zhao *et al.*, 2014; Prakash *et al.*, 2016). According to the poisoning of carbon monoxide produced from the dehydration of formic acid which leads to a decreasing activity of the metal catalyst, the second metal, such as, Ru, or Sn, is added into metal catalyst to reduce interaction between the metal catalyst and carbon monoxide (Gasteiger *et al.*, 1996; Wang *et al.*, 1996; Hayden *et al.*, 2003; Haan *et al.*, 2010; Stevanović *et al.*, 2014). Therefore, we attempt to apply Ni, as base metal, to tin in order to utilize as a second metal due to cost, non-toxicity, abundance in nature, and ability to transfer its electron filling d-band vacancies of Ni leading to an increase electron density of Ni metal (Swift *et al.*, 1968).

Bimetallic catalysts could be prepared by various methods, for example vapor deposition, impregnation, co-precipitation, liquid-phase synthesis, and mechanical alloying (Asedegbega-Nieto *et al.*, 2006; Liu *et al.*, 2010; Wei *et al.*, 2012). In this work, mechanically alloyed (MAed) Ni_xSn_y intermetallic catalysts were focused since they are not only easy to prepare and control nanoparticle size, but also low cost. For kinetic study, the catalyst activity and selectivity were considered. The studied factors that might affect to the activity and the selectivity are type and amount of catalyst, solvent type, temperature and time, and ratio of the reactants (CALD : FA) to achieve maximum yield of COL conversion.

CHAPTER II
LITERATURE REVIEW

2.1 Hydrogenation of Cinnamaldehyde

In CALD, hydrogenization can occur at either C=C, C=O, or both positions to either HCALD, COL, or HCOL, respectively (Figure 2.1). The most important desirable product for industry is COL. Therefore, the selectivity to COL should be considered.

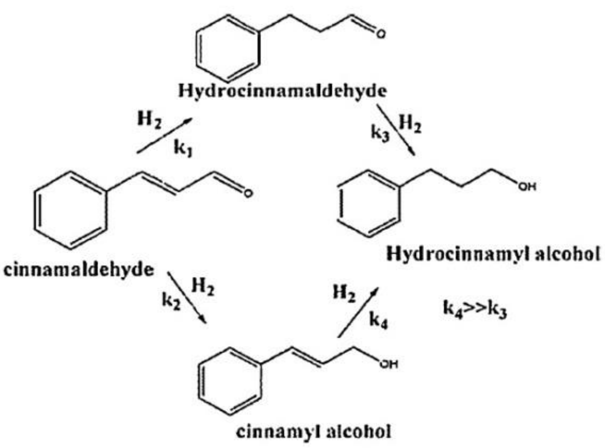

Figure 2.1 Hydrogenation of CALD reaction pathways (Prakash *et al.*, 2016).

The selectivity to COL is mostly determined in term of the competitive adsorption between C=C and C=O bonds on the metal surface. Figure 2.1 shows the possible adsorption structures of theα, β-unsaturated aldehyde molecules which are strongly dependent of the nature of the metal and the direction of the molecular adsorption. For example, (Delbecq *et al.*, 1995) studied the adsorption of various α,β-unsaturated aldehydes on Pt and Pd crystal surfaces using semi-empirical extended Hϋckel calculation. They revealed that a di-σ form was preferred on Pt {111}, a planar η4 form on Pd {111}, and Pt {100}, and a πC=C form on Pt {110}. Thus, the selectivity could be improved by predominantly increasing the hydrogenation of the adsorption direction at C=O bond (Gallezot *et al.*, 1998). See Figure 2.2.

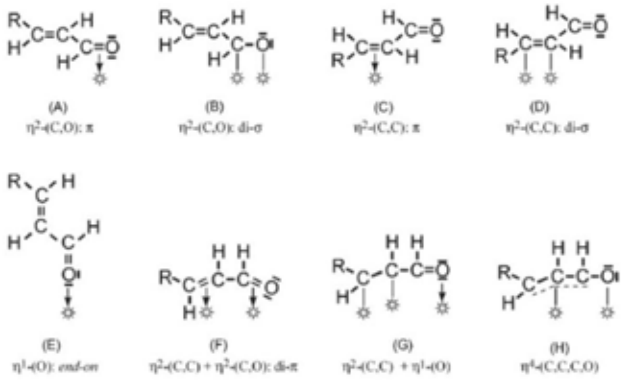

Figure 2.2 Possible structures obtained from adsorption of α, β-unsaturated aldehydes (Santori *et al.*, 2002).

2.2 Hydrogen Generation from Formic Acid

FA, a non-toxic liquid, has been widely used as a hydrogen source in hydrogenation reaction because it is not only easy handling and transportation, but also containing 4.4 %wt hydrogen. Two principal decomposition pathways are shown in eq. 1-2 (Yadav *et al.*, 2012).

$$HCOOH \longrightarrow H_2 + CO_2 \qquad \Delta G = -48.4\ kJ/mol \qquad (1)$$

$$HCOOH \longrightarrow H_2O + CO \qquad \Delta G = -28.5\ kJ/mol \qquad (2)$$

Equation 1, producing H_2 and CO_2, is the desired reaction in this study. A simple pathway observed for the selective decomposition of FA to H_2 and CO_2 on the metal surface is shown in Figure 2.3. The formate route plays an important role and the rate-determining step is the dissociation of formate to CO_2 and hydrogen intermediate species on metal catalyst surface (H). The most adsorption configuration of formate has a O-bidentate bridging structure (Singh *et al.*, 2016).

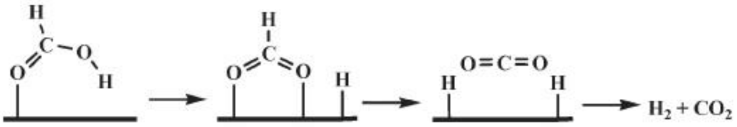

Figure 2.3 General mechanism of formic acid decomposition over various surfaces through formate route (Singh *et al.*, 2016).

2.3 Selectivity of Cinnamyl Alcohol

As mentioned previously, the selectivity of COL is determined by the competitive adsorptions between C=C and the C=O bonds on the metal surface (Gallezot *et al.*, 1998). The selectivity could be improved by not only decreasing the binding energy of the C=C bond due to the increase of the repulsive four-electron interactions with the metal, but also adding Lewis acid sites onto the catalyst, leading to activated C=O bond. Essentially, the optimal conditions need to be considered to improve selectivity of COL.

2.3.1 Solvent

The most important factors affecting the hydrogenation of α, β-unsaturated aldehydes are solvent polarity, FA decomposition, interaction between the catalyst and the solvent, and solvation of reactants in liquid phase (Zhang *et al.*, 1998; Pham-Huu *et al.*, 2001; Hájek *et al.*, 2003; Mäki-Arvela *et al.*, 2005; Liu *et al.*, 2015). Influence of solvent had been studied by using iron-based catalyst system, consisting of $Fe(BF)_4{\cdot}6H_2O$ and $P(CH_2CH_2PPh_2)_3$ at 40 °C for 2h, ambient pressure, and the results are shown in Table 2.1 (Wienhöfer *et al.*, 2013).

Table 2.1 Influence of solvents on selective hydrogenation of cinnamaldehyde (Wienhöfer *et al.*, 2013)

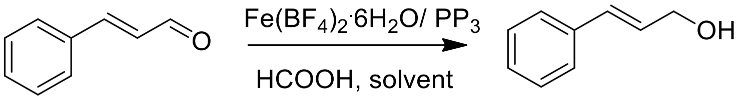

Entry	**Solvent**	**Conversion[%]**	**Cinnamyl alcohol yield[%]**	**Selectivity[%]**
1	Toluene	-	-	-
2	MeOH	70	5	7
3	*i*-PrOH	25	16	64
4	THF	31	31	99
5	EtOH	48	16	33
6	2-Me-THF	9	9	99
7	*t*-AmOH	14	14	99

*Reaction conditions: 0.5 mmol CALD, 0.75mol% catalyst loading, 1ml of solvent, 2 eq. of FA, 40 °C, 2h

Table 2.1 shows that using tetrahydrofuran as a solvent achieved 99% selectivity of COL. In contrast, methanol gave 70% conversion with 5% COL yield. Likewise, EtOH gave 48% conversion and 16% yield of COL due to the side reaction of acetalization in alcohol solvent giving hemiacetals and acetals which were undesirable products (Wienhöfer *et al.*, 2013). In addition, the reaction could hardly occur when toluene was used as a solvent because of its polarity.

Similarly, the experiment using *im*-Pt/SiO_2, prepared by impregnation, followed by reduction at 400 °C, as catalyst under 4.9 MPa H_2, 50 °C and 2 h reaction time revealed that MeOH gave a maximum conversion with acetal by-product. Other kinds of solvent provided lower conversion with decreasing solvent polarity in the order of EtOH > 2-pronanol > cyclohexane. However, these solvents did not give other by-products, HCALD and HCOL, as shown in Figure 2.4 (Shirai *et al.*, 2001).

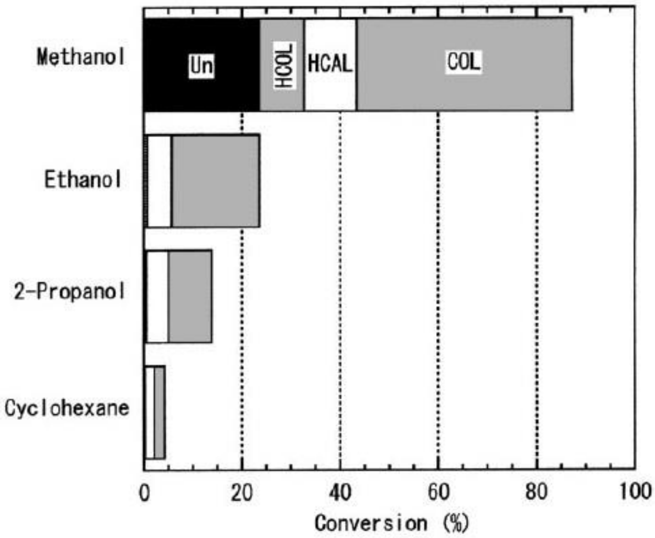

Figure 2.4 Results of CALD hydrogenation with *im*-Pt/SiO_2(400) in different solvents at 120 min reaction time, 4.9 MPa, 0.16 mol/L CALD concentration (Shirai *et al.*, 2001).

2.3.2 Time and Temperature

Generally, the product increases with increasing time. Hydrogenation of CALD using *im*-Pt/SiO_2 (400) prepared by impregnation followed by reduction at 400 °C as a catalyst in EtOH at 6.9 MPa and 50 °C indicated that COL and HCALD were produced as CALD was disappearing. The amount of COL increased with time and became constant when CALD was completely consumed. The amount of HCOL increased as a function of time. Moreover, it was found that HCOL was produced mostly from HCALD during CALD hydrogenation when HCALD remained, as shown in Figure 2.5 (Shirai *et al.*, 2001).

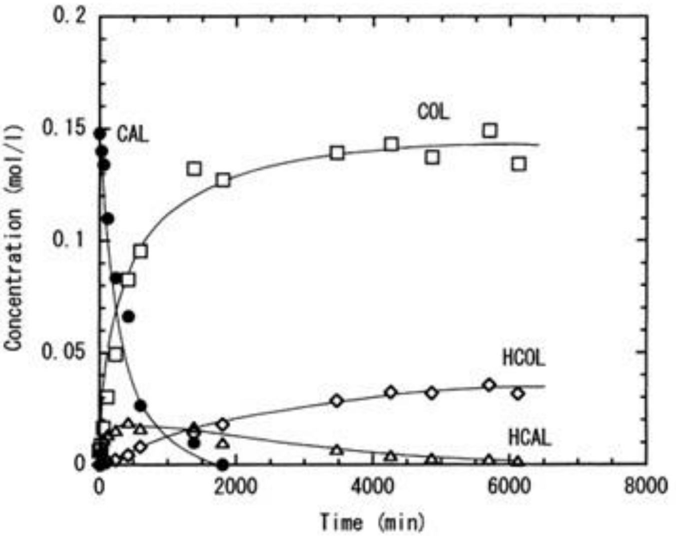

Figure 2.5 Changes of reactant and product concentrations during CALD hydrogenation with *im*-Pt/SiO_2(400) in EtOH at 6.9 MPa H_2 and 0.16 mol/L CALD concentration (Shirai *et al.*, 2001).

As for the reaction temperature, by using $Fe(BF_4)_2{\cdot}6H_2O/PP_3$ as a catalyst, 2 equivalents of formic acid as a hydrogen source, the reaction temperature had a major influence on the reactivity of the system. While changing temperature from 20° to 40 °C, the conversion was raised from 11 to 31%, a further increase to 60 °C led to 100% conversion for the same reaction time (Wienhöfer *et al.*, 2013).

2.3.3 Type of Catalyst

Due to high costs of Pt and Pd, Ni, a Pt-group metal and cheaper material, is a worthy material to utilize as a hydrogenation catalyst. Unfortunately, hydrogenation on metal surface (such as, Ru, Pt, Rh, Cu, or Ni) at C=C bond which is the undesired reaction is easier to occur than that at C=O bond (Gallezot *et al.*, 1998). Thus, selectivity to hydrogenation at C=O bond need to be considered. One of the most effective methods to increase hydrogenation at C=O bond was to incorporate a second more electropositive metal to activate the C=O bond that leads to higher tendency in generating unsaturated alcohol (Prakash *et al.*, 2016). For example, hydrogenation of CALD using tin-modified platinum-based catalysts was studied at 40 °C, 1 MPa H_2 in isopropanol solvent. This study revealed that in the case of the monometallic catalyst (Pt), the major product was the HCALD while COL was maintained at 20% selectivity. The addition of tin (PtSn) at the same condition resulted in more than twice higher activity and higher selectivity to COL over 35% selectivity (Santori *et al.*, 2002). The FA dehydrogenation on Ni was also studied (Luo *et al.* 2012; Luo *et al.*, 2013) and revealed that FA preferred the O of O=C to form H bridging (H=O) with two neighboring nickel atoms, and formate preferred the bidentate adsorption with O atoms atop on nickel surface.

2.3.4 Amount of Catalyst

From previous studies, we knew that the rate of the reaction was affected by number and rearrangement of sites on metal. Thus, not only type of catalyst, but also amount of catalyst loaded into the system play an important role to control the rate of the reaction. Wienhöfer and coworkers studied hydrogenation of α, β-unsaturated aldehydes using iron-based catalyst system, consisting of $Fe(BF)_4 \cdot 6H_2O$ and $P(CH_2CH_2PPh_2)_3$. In the case of CALD, they found that the conversion and COL yield increased with increasing catalyst loading while the selectivity was practically constant, more than 99% selectivity, as can be seen in Table 2.2. In addition, by using higher catalyst loading, they could obtain shorter reaction time (Wienhöfer *et al.*, 2013).

Table 2.2 Influence of catalyst loading on selective hydrogenation of CALD (Wienhöfer *et al.*, 2013)

Entry	**Catalyst loading [mol%]**	**Conversion [%]**	**COL yield [%]**	**Selectivity [%]**
1	0.2	20	20	>99
2	0.3	31	31	>99
3	0.4	40	40	>99
4	0.5	100	>99	>99
5**	0.4	100	>99	>99
6***	2.0	100	>99	>99

*reaction conditions: 0.5 mmol CALD, 1ml THF, 2 eq. formic acid, 60°C, 2h

** reaction condition: 1.1 eq. formic acid

*** reaction condition: 10 min

2.3.5 Ratio of Reactants

Typically, stoichiometric ratio affects to the rate of the reaction and how significant the ratio impacts the reaction rate can be determined by the rate law, including order of the reaction and concentrations of the reactants. Apart from varying amount of catalyst, Wienhöfer and coworkers also studied the reactant ratio by varying the ratio of CALD to FA and the results in Table 2.3 showed that using lower amounts of formic acid led to incomplete conversion whereas use of one equivalent of FA provided the best results (Wienhöfer *et al.*, 2013).

Table 2.3 Influence of CALD to FA ratio on selective hydrogenation of CALD (Wienhöfer *et al.*, 2013)

Entry	**Ratio of CALD : FA**	**Conversion[%]**	**COL yield[%]**	**Selectivity[%]**
1	1 : 0.75	75	75	>99
2	1 : 1	97	97	>99
3	1 : 1.25	83	83	>99
4	1 : 1.5	60	60	>99

*Reaction conditions:0.5 mmol CALD, 0.3 mol% catalyst loading, 1ml of THF, 60 °C,2h

CHAPTER III
EXPERIMENTAL

3.1 Materials

Ni powder (Ni, 99.99 %wt) was purchased from Sigma Aldrich Chemical Co. Inc., USA and Sn powder (Sn, 99.99 %wt) was produced using gas atomization (Morakotjinda *et al.*, 2010). *Trans*-Cinnamaldehyde, cinnamyl alcohol, hydrocinnamaldehyde, hydrocinnamyl alcohol, and formic acid were purchased from Sigma Aldrich Chemical Co. Inc., USA. Tetrahydrofuran, dioxane, and chlorobenzene were bought from RCI Labscan Limited. All chemicals were used without purification.

3.2 Equipment

X-ray diffactometry (XRD, Rigaku X-ray diffactometer with CuKα radiation, λ= 0.154 Å) was used to identify phase of Ni_xSn_y intermetallics using a scanning speed of 1 degree/min with the range of 2θ equal to 20°–80°. Field emission scanning microscopy/energy dispersive X-ray analysis (FE-SEM-EDS) element mapping was used to assured the uniformity of Ni and Sn compositions. For catalytic activity study, existing chemicals were detected by gas chromatography - flame ionization detector (GC-FID), using a capillary column ZB-5MS (30 m x 250 µm x 0.5 µm, Agilent Technologies, USA) with 1 µL injection volume, a 1.0 mL/min flow rate, 110 °C column temperature, and 9 min run time condition. Ammonia Temperature programmed desorption (NH_3-TPD, BELCAT II, BEL Japan Inc.) was used to determine acid sites number of Ni_xSn_y intermetallics and the oxidation states of Sn were identified by X-ray photoelectron spectroscopy (XPS) using AXIS ULTRA^{DLD} spectrometer.

3.3 Methodology

3.3.1 Catalyst Preparation by Mechanical Alloying Method

Various Ni (32 ≤ µm) powder contents were mixed with various contents of 30, 50, 70, and 100 %wt Sn (32 ≤ µm) powder in an attritor. The mixture was milled using the following conditions: 5:1 ball-to-powder ratio, 300 rpm MA speed, and 30h milling time. The mixture was heated in a vacuum chamber and further characterized by XRD to determine phase of intermetallics (Pithakratanayothin *et al.*, to be submitted).

3.3.2 Effect of Solvent Type

Ni_3Sn (300 mg) was placed in a round bottom flask with various solvents, THF and 1, 4-dioxane (10ml). The flask was then refluxed, stirred, and heated up to 60°C. CALD (630 µL, 5mmol) and FA (25 µL per 5 min) were added into the solution for 5 h reaction time. The solution was taken for GC-FID analysis.

3.3.3 Effects of Reaction Time and Temperature

3.3.3.1 Influence of Reaction Temperature

300 mg of Ni_3Sn was placed in a round bottom flask with THF. The flask was then refluxed, stirred, and heated up to various temperatures, 50°, 60°, 70°, and 80°C. CALD (630 µL, 5mmol) and FA (25 µL per 5 min) were added into the solution for 5 h reaction time. The solution was taken for GC-FID analysis.

3.3.3.2 Influence of Reaction Time

300 mg of Ni_3Sn was placed in a round bottom flask with THF. The flask was then refluxed, stirred, and heated up to 60 °C. CALD (630 µL, 5mmol) and FA (25 µL per 5 min) were added into the solution. The experiment was carried out until the conversion did not change after checking with GC-FID analysis.

3.3.4 Effect of Catalyst Type

300 mg of various Ni_xSn_y (Ni_3Sn, Ni_3Sn_2, and Ni_3Sn_4) was placed in a round bottom flask with THF. The flask was then refluxed, stirred, and heated up to 60°C. CALD (630 µL, 5mmol) and FA (25 µL per 5 min) were added into the solution for 5 h reaction time. The solution was taken for GC-FID analysis.

3.3.5 Effect of Amount of Catalyst

Various amount of Ni_3Sn_4 (150, 300, and 900 mg) was placed in a round bottom flask with THF. The flask was then refluxed, stirred, and heated up to 60°C. CALD (630 µL, 5mmol) and FA (25 µL per 5 min) were added into the solution for 3 h reaction time. The solution was taken for GC-FID analysis.

3.3.6 Effect of FA Adding Rate

300 mg of Ni_3Sn_4 was placed in a round bottom flask with THF. The flask was then refluxed, stirred, and heated up to 60°C. CALD (630 µL, 5mmol) and FA with different adding rate (10 µL per 2 min, 25 µL per 5 min, and 900 µL) were added into the solution for 3 h reaction time. The solution was taken for GC-FID analysis.

CHAPTER IV
RESULTS AND DISCUSSION

4.1 Characterization of Ni_xSn_y Intermetallics

The Ni_xSn_y intermetallics were characterized by XRD at the range of 20° to 80°. The results showed that different metal powder ratios of nickel to tin led to different formulas of Ni_xSn_y intermetallics. From XRD patterns, Figure 4.1 showed single phase of Ni_3Sn_4 (ICDD-DB card number 03-065-4553), Ni_3Sn_2 (ICDD-DB card number 03-065-9460), and Ni_3Sn (ICDD-DB card number 01-073-4993). When the metal powder ratio of nickel to tin was equal to 1.33, Ni_3Sn was successfully prepared whereas Ni_3Sn_2, and Ni_3Sn_4 were synthesized when metal powder ratios were 0.72 and 0.33, respectively. The XRD pattern of the higher Sn contents, such as Ni_3Sn_4, showed more high-index planes. Ramos de Debiaggi and coworkers (2013) studied some lattice parameters of Ni-Sn intermetallics using *ab initio* density-functional-theory (DFT) method with the exchange and correlation functions studied by Perdew and Wang in the generalized gradient approximation (GGA) and also by Ceperley and Alder in the local-density-approximation (LDA), see Table 4.1. The calculations revealed that changing in the Sn composition led to the changing in the lattice parameters and the equilibrium volume. This is due to the lattice expansion insisting Sn, meaning that the higher Sn content resulted in the higher lattice constant and the equilibrium volume. The FE-SEM-EDX element mapping assured the uniformity of Ni and Sn compositions (Figure 4.2). In addition, the oxidation states, Sn^{4+} and Sn^{2+} of Sn, were identified by X-ray photoelectron spectroscopy (XPS). The Sn $3d_{5/2}$ spectra revealed the peaks as following; Sn^{4+} of Ni_3Sn was 486.2 eV, Sn^{4+} and Sn^{2+} of Ni_3Sn_2 were 487.2 eV (86.8%) and 485.8 eV (13.2%), and Sn^{4+} and Sn^{2+} of Ni_3Sn_4 were 487.4 eV (80.0%) and 485.6 eV (20.0%), respectively. These XPS results corresponded to the metal-metal bond was formed by Ni-Sn mechanical alloying due to the shifting of Sn binding energy (485.0-485.5 eV) and the Sn binding energy peaks that shifted to higher binding energies related to electron transfers from Sn to Ni (Chen *et al.*, 2012). See Figure 4.3.

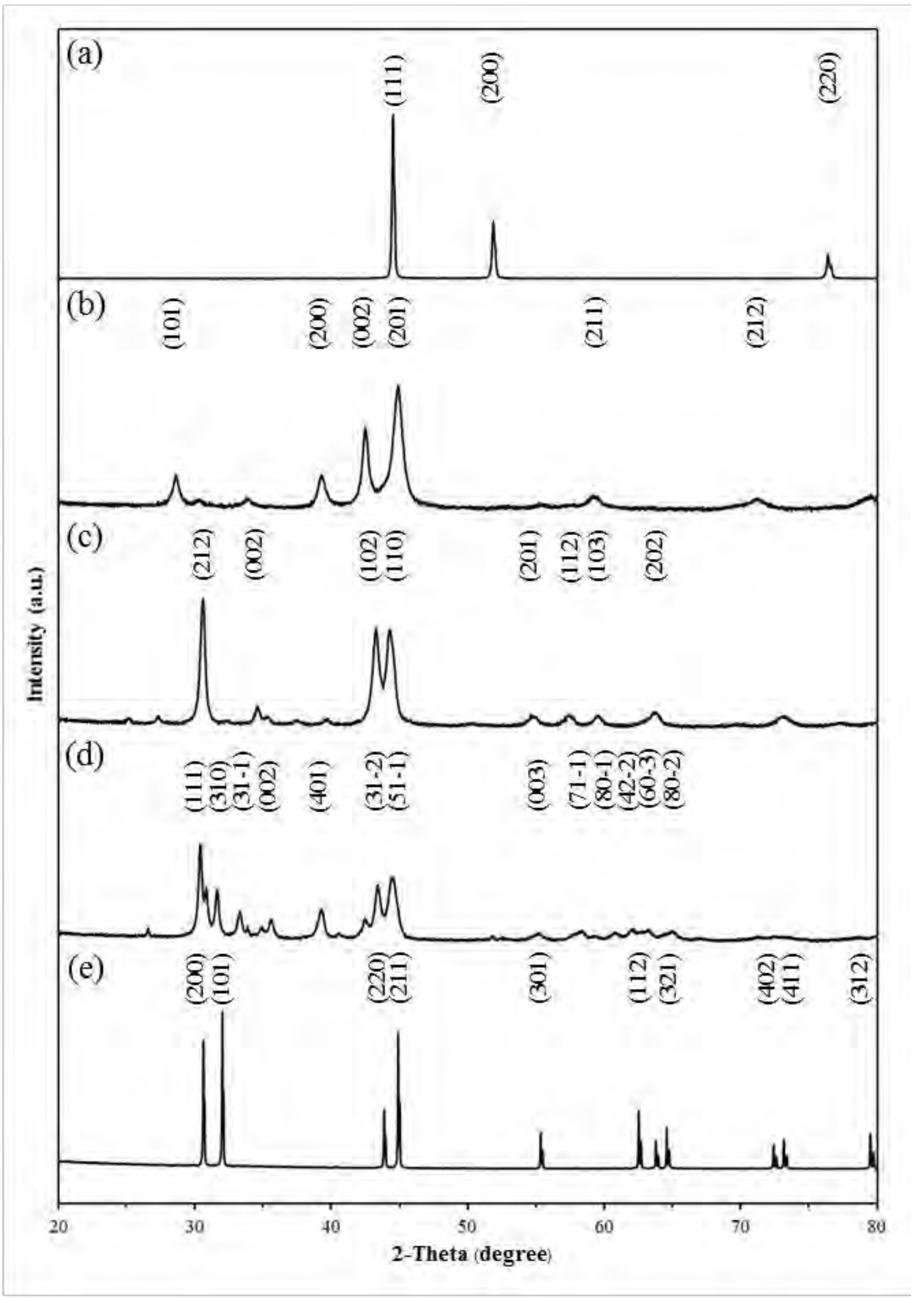

Figure 4.1 XRD patterns of (a) Ni, (b) Ni_3Sn, (c) Ni_3Sn_2, (d) Ni_3Sn_4, and (e) Sn.

Table 4.1 The lattice parameters (in Å) and the equilibrium volume, V_0, (in Å^3/atom) of Ni-Sn intermetallics at 0 K calculated by *ab initio* density-functional-theory (DFT) method with the exchange and correlation functions of Perdew and Wang in the generalized gradient approximation (GGA) and also Ceperley and Alder in the local-density-approximation (LDA) (Ramos de Debiaggi *et al.*, 2013)

Phase	Pearson Symbol	a, b, c	V_0	Approx.
Ni	cF4	3.425	10.044	LDA
		3.523	10.931	GGA
Ni_3Sn	hP8	5.181, 4.153	12.065	LDA
		5.317, 4.255	13.021	GGA
Ni_3Sn_2	oP20	6.985, 5.094, 7.991	14.217	LDA
		7.164, 5.228, 8.213	15.381	GGA
Ni_3Sn_4	mC14	12.024, 3.988, 5.131	16.971	LDA
		12.312, 4.087, 5.266	18.304	GGA
Sn	tI4	5.794, 3.121	26.193	LDA
		5.948, 3.204	28.348	GGA

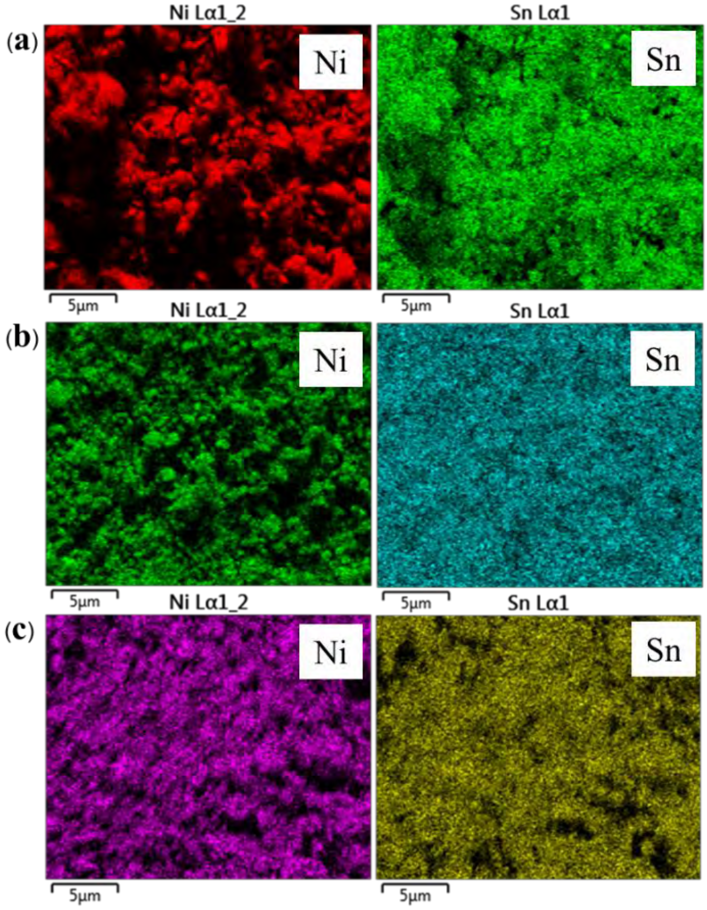

Figure 4.2 FE-SEM-EDX elemental mapping images of (a) Ni_3Sn, (b) Ni_3Sn_2, and (c) Ni_3Sn_4.

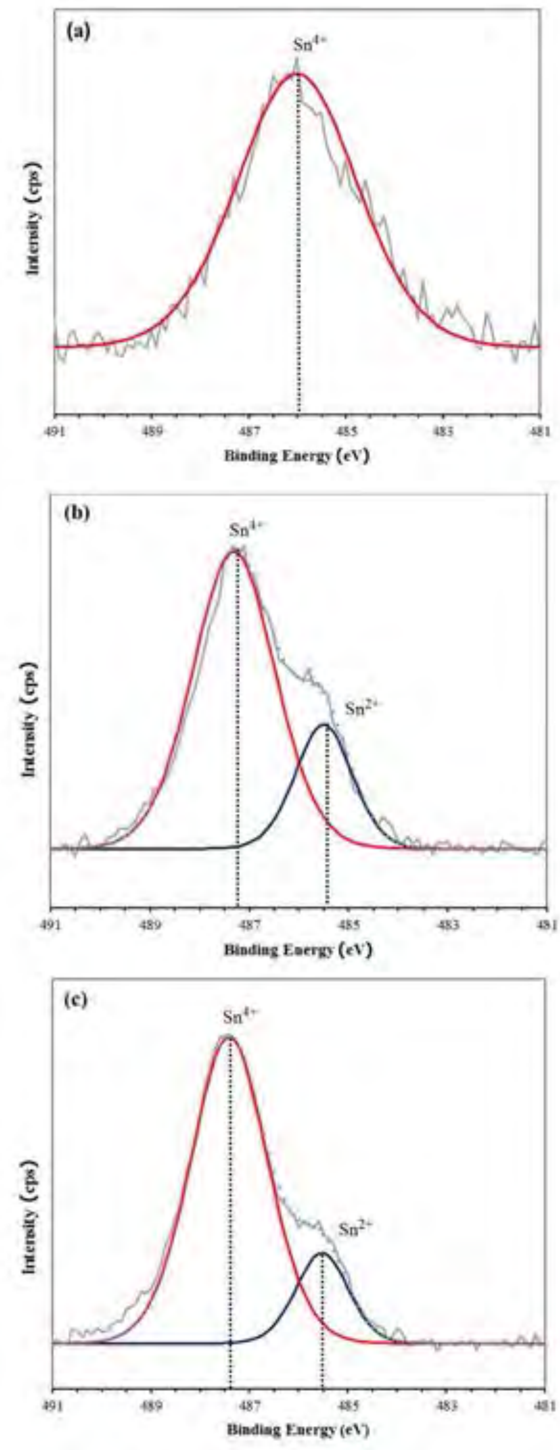

Figure 4.3 Sn $3d_{5/2}$ spectra of (a) Ni_3Sn, (b) Ni_3Sn_2, and (c) Ni_3Sn_4.

4.2 Solvent Effect

Properties of solvent are to help the miscibility of reactants and do not react with the reactants. Protic solvents, such as methanol, ethanol, and isopropanol, can lead to acetal or hemi-acetal products (Hájek *et al.*, 2003), see Figure 4.4.

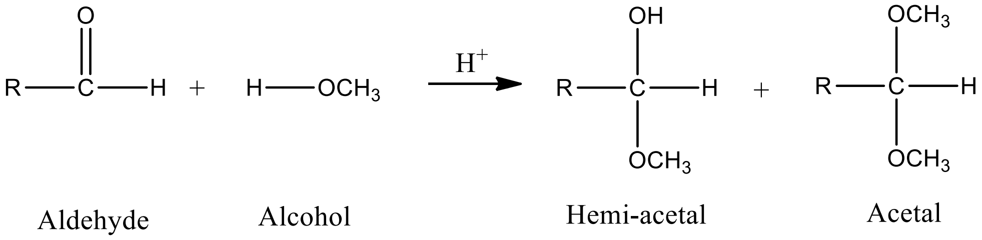

Figure 4.4 Scheme of hemi-acetal and acetal formation (Hájek *et al.*, 2003).

Thus, they were disregarded to be involved in the reaction as solvents. Both tetrahydrofuran (THF), which has 7.5 of dielectric constant, and 1, 4-dioxane, which has 2.3 of dielectric constant, were therefore chosen as polar and non-polar aprotic solvents, respectively, to study how polarity of solvent affect to the system.

Figure 4.5 shows that both THF and dioxane solvents did not give much different conversions along 5 h reaction time. Although the solvent polarity was reported that it affected to hydrogenation rates (Hájek *et al.*, 2003; Liu *et al.*, 2015), conversion of CALD did not clearly differ due to the side reactions of benzaldehyde via retro-aldol condensation and cinnamic acid via oxidation (Chen *et al.*, 2010; Marteau *et al.*, 2013, Yadav *et al.*, 2013), see Figure 4.6, occurring in both solvents. The effect of solvent was obviously noticed by the yield of COL (Figure 4.7). By using THF as solvent, we obtained higher yield of COL comparing with using dioxane because solvent not only homogenized the system but also polarized chemical bonding meaning that THF, polar solvent, polarized C=O bond leading to activated C=O position and hydrogenation at aldehyde group.

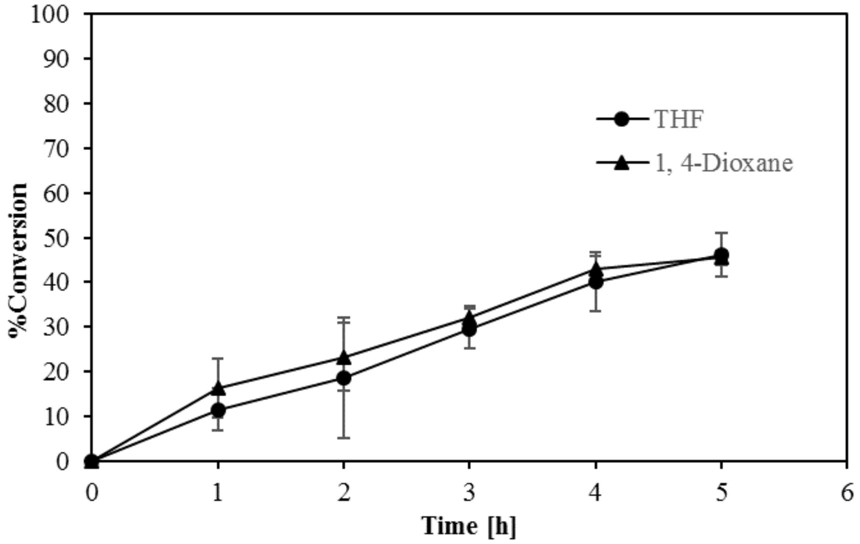

Figure 4.5 Plots of conversion versus time using THF and 1, 4-dioxane as solvents; 300 mg of Ni_3Sn, 60 °C, 5 mmol CALD, 25 µL of FA per 5 min, 10mL of solvent.

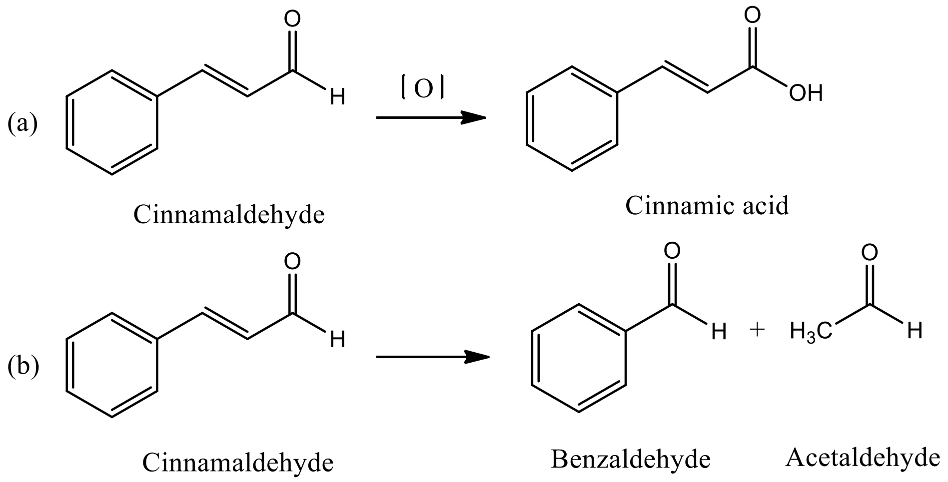

Figure 4.6 Scheme of (a) cinnamaldehyde oxidation to cinnamic acid, and (b) retro-aldol condensation of cinnamaldehyde to benzaldehyde (Yadav *et al.*, 2013).

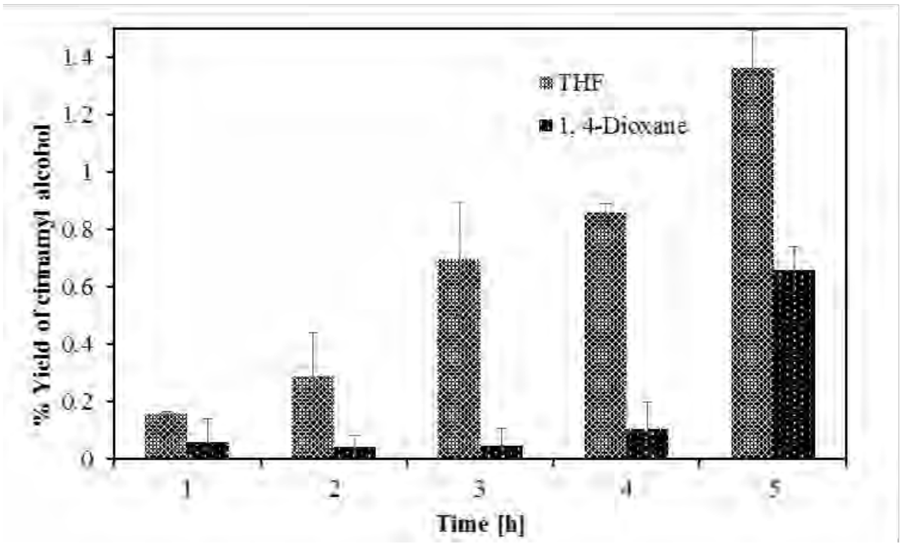

Figure 4.7 Plots of the yield of COL versus time using THF and dioxane as solvents; 300 mg of Ni_3Sn, 60 °C, 5 mmol CALD, 25 μL of FA per 5 min, 10 mL of solvent.

Since, in this work, our desired product was COL, THF was, thus, chosen to be the solvent for further study.

4.3 Time and Temperature Effects

4.3.1 Effect of Temperature

It is known that the reaction temperature may affect both conversion and chemoselectivity in hydrogenation of α, β-unsaturated aldehyde (Koo-amornpattana *et al.*, 2001; Liu *et al.*, 2015). Therefore, the reaction temperature was needed to study. Due to the boiling point of THF which is 65 °C, the temperature was varied from 50° to 80 °C and the conversion was shown in Figure 4.8.

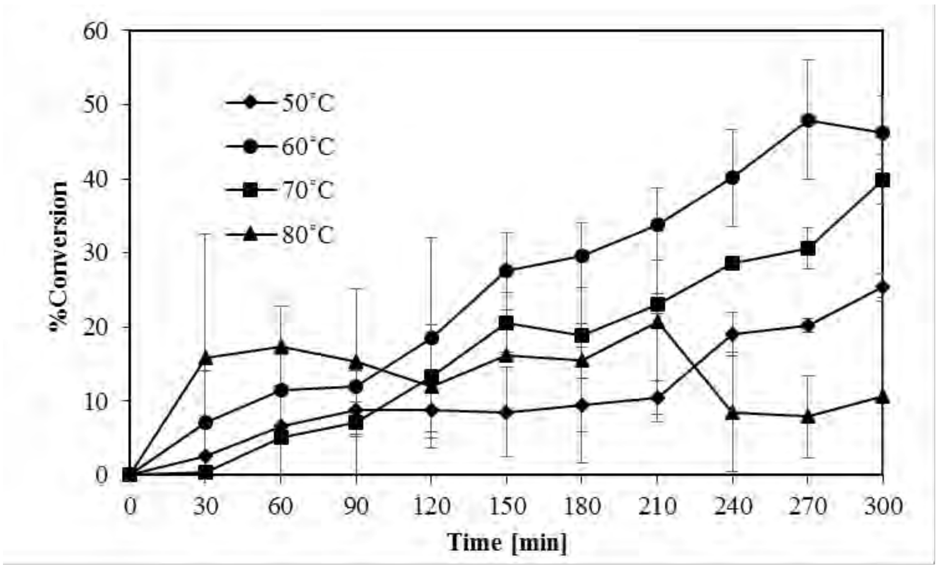

Figure 4.8 Conversion of CALD versus time using various reaction temperatures; 300 mg of Ni_3Sn, 5 mmol CALD, 25 μL of FA per 5 min, 10mL of THF.

Reaction temperature of 60 °C provided the highest conversion, as compared to the other studied temperatures, meaning that this temperature was proper to grow the reaction. At the first 1.5 h, the conversion of 80 °C showed the highest conversion, but then decreased to the lowest when the time passed. This behavior occurred because THF was rapidly boiled and condensed back and forth leading to the conversion fluctuation of 80 °C, meaning that this temperature was too high to conduct the reaction. Reaction temperature of 70 °C gave a higher conversion than 50° and 80 °C. From the obtained results, we decided to study the optimal time of the reaction at 60 °C reaction temperature.

4.3.2 Effect of Reaction Time

Figure 4.9a revealed that the conversion considerably increased after 5 h at 44%, then slightly increased to 67% conversion at 12 h. Finally, the conversion was constant after 12 h. Since our desired product was COL, we considered not only conversion, but also selectivity and yield of COL. We found that COL continuously increased until the fifth hour, then the yield of COL reduced because it was probably converted to other products, such as HCALD, β-methyl styrene, 1-propylbenzene, or aldol condensation product (Hájek *et al.*, 2003), see Figure 4.9b.

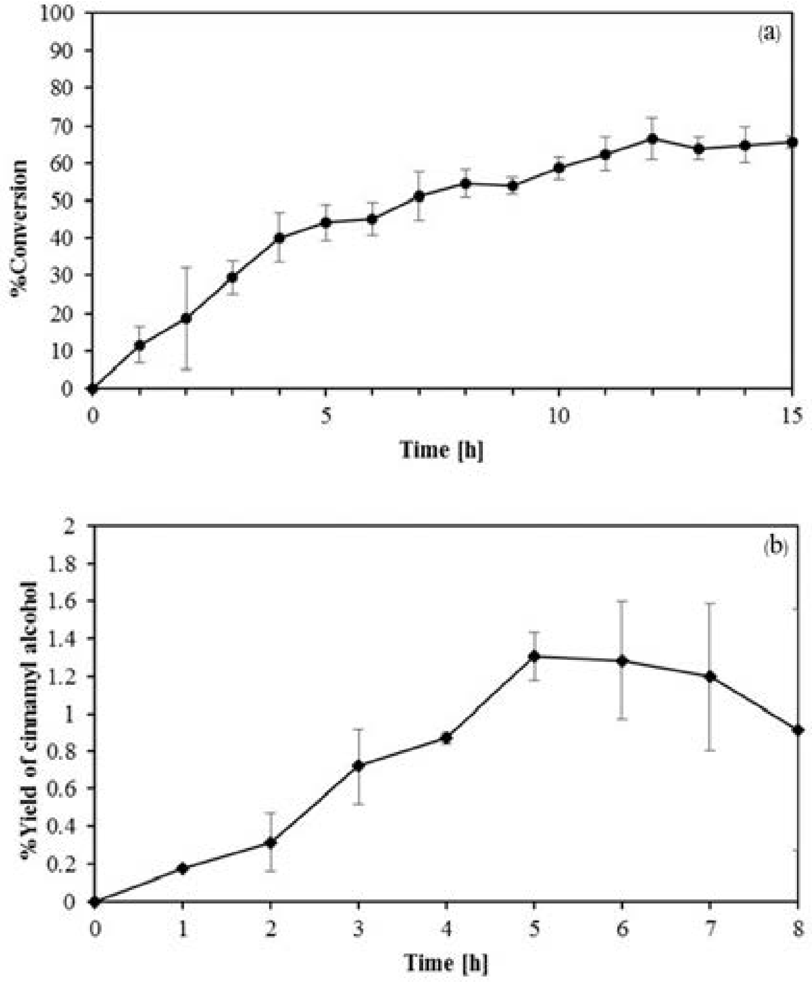

Figure 4.9 Plots of (a) CALD conversion, and (b) yield of COL versus time; 300 mg Ni_3Sn, 5 mmol CALD, 25 μL FA per 5 min, 60 °C, 10 mL THF.

Since the conversion significantly increased until the fifth hour and the maximum yield of COL was also detected at that time, therefore, the next factor was investigated using all of optimal conditions, as discussed earlier, including THF as solvent at 60 °C for 5 h reaction time, to observe how tin content in the Ni_xSn_y intermetallics affected to the reaction.

4.4 Type of Catalyst Effect

To study the effect of the Sn content, type of catalyst was varied while fixing the other parameters. Evidently, the higher Sn content resulted in the higher turnover number (TON), as can be seen in Figure 4.10, showing the TON order as following; Ni_3Sn (2.2) < Ni_3Sn_2 (3.2) < Ni_3Sn_4 (5.8). These results indicated that interstitial Sn expanded the lattice and changed the crystal system and other lattice parameters with high-index planes (see Table 4.1 and Figure 4.1) and its low coordination sites which related to the greater activity (Wang *et al.*, 2011; Chen *et al.*, 2012). Generally, only Sn itself is inactive for hydrogenation (Rodiansono *et al.*, 2012), but the activity of the Sn in this system was achieved due to a help of formic acid, protonating the starting cinnamaldehyde and forcing the reaction to move forward.

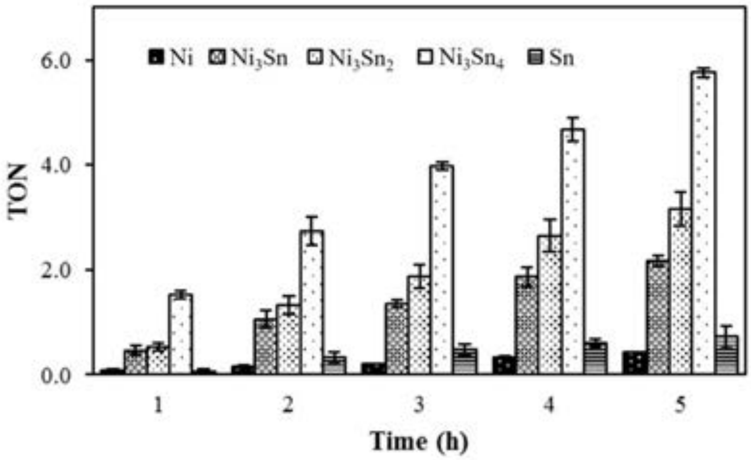

Figure 4.10 Plots of turnover number (TON) versus time of various Ni_xSn_y intermetallics, Ni, and Sn powders using 5 mmol CALD, 25 µL of FA per 5 min with THF at 60 °C.

Generally, hydrogenation of α, β-unsaturated aldehyde under mild conditions was attractive and challenging, the focused products in this study was undergone via hydrogenation. The selectivity of the hydrogenation pathway were

4.0, 3.4, and 7.8% for Ni_3Sn (hexagonal) , Ni_3Sn_2 (hexagonal) , and Ni_3Sn_4 (monoclinic), respectively, meaning that the crystal system had an influence on the reaction pathway and the hexagonal structure of Ni_3Sn and Ni_3Sn_2. The number of acid sites determined by NH_3-TPD showed an increase in the number of active sites with increasing the Sn content as following; Ni_3Sn_4 (1.302 mmol/g) > Ni_3Sn (0.702 mmol/g) ≃ Ni_3Sn_2 (0.693 mmol/g) > Ni (0.129 mmol/g). This evidence was related to cinnamyl alcohol product (see Figure 4.11), the hydrogenation at C=O bond, due to the interaction of lone pair electrons and the acid sites on metal surface. In this work, COL was desired product because hydrogenation at C=O bond of α, β-unsaturated aldehyde was interesting due to the reasons that have been mentioned earlier. Hydrocinnamaldehyde was also obtained because Ni which was electronegative composition might create repulsive force with oxygen atom at C=O bond, leading to C=C bond adsorption instead. In addition, further hydrogenation resulted in hydrocinnamyl alcohol product. In this condition, benzaldehyde and cinnamic acid were found as products at high yield (Marteau *et al.*, 2013; Yadav *et al.*, 2013), see Table 4.2. Moreover, the COL yields at 3, 4, and 5 h reaction times were 1.83, 1.87, and 2.03 % by using Ni_3Sn_4 intermetallics at 60 °C, respectively. Therefore, 3 h reaction time was the optimal reaction time for cinnamyl alcohol production, as shown in Figure 4.11.

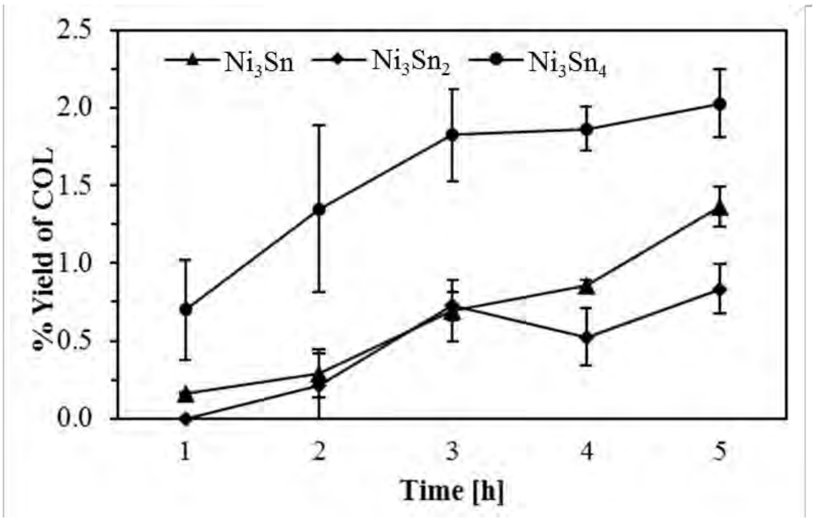

Figure 4.11 Yield percentage of COL using Ni_xSn_y intermetallics, 5 mmol CALD , 25 μL of FA per 5 min with 10 mL THF at 60 °C.

Table 4.2 Selectivity Percentage of all products using various catalysts, 5 mmol cinnamaldehyde, 25 μl of FA per 5 min, 60 °C, 5 h, 10 ml of THF

Catalyst	**Desired series**			**Other products**	
	COL	**HCALD**	**HCOL**	**Benzaldehyde**	**Cinnamic acid**
Ni	4.5	0.0	0.6	53.2	41.6
Ni_3Sn	2.9	1.1	0.0	58.6	37.3
Ni_3Sn_2	1.9	1.4	0.1	69.6	26.9
Ni_3Sn_4	3.7	2.0	2.1	56.5	35.8
Sn	2.3	0.0	0.0	58.1	39.6

4.5 Amount of Catalyst Effect

Another way to maximize COL yield or force the reaction undergoing faster was to increase the number of active sites that had an impact on the amount of the reactant that interacted on the catalyst surface. For this reason, the catalyst amount was investigated.

Since the selective hydrogenation of α, β-unsaturated aldehyde was remarkably challenging, hydrogenation products was mainly concerned. By loading 150 and 900 mg of Ni_3Sn_4, conversions obtained were lower than that obtained using 300 mg of Ni_3Sn_4 (25.2%) due to too small (150 mg) and too high (900 mg) amounts of the catalyst, causing too low and too much active sites, respectively. Too much catalyst provided too much number of active sites and led to not only rapid decomposition of formic acid but also a decrease in the active site by formic acid, resulting in a smaller amount of cinnamaldehyde to interact with the catalyst (Singh *et al.*, 2016). See Figure 4.12.

Moreover, the other hydrogenation pathway products, HCALD and HCOL, showed the same tendency as COL due to the same reasons. Benzaldehyde and cinnamic acid were found as by-products at high yield, see Table 4.3.

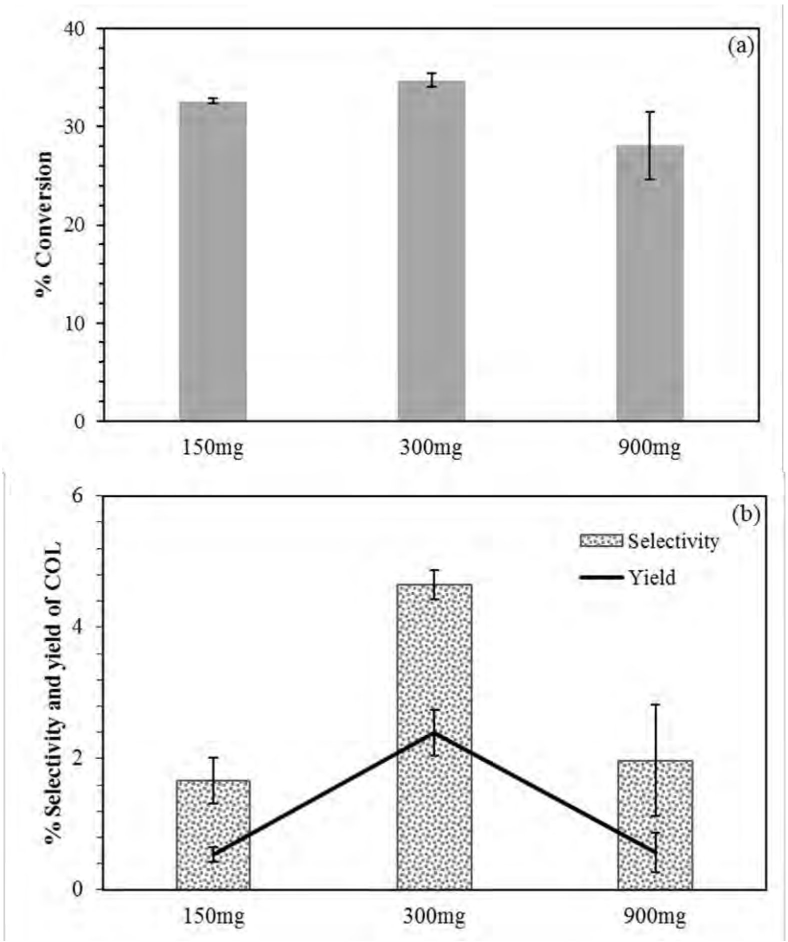

Figure 4.12 Plots of (a) overall conversion of CALD, and (b) selectivity and yield of COL with various amount of Ni_3Sn_4 as catalyst using 5 mmol CALD, 25 µL FA per 5 min with THF at 60˚C and 3 h reaction time.

Table 4.3 Selectivity percentage and yields of all products using various amounts of Ni_3Sn_4, 5 mmol CALD, 25 µL of FA per 5 min with THF at 60 °C for 3 h

Ni_3Sn_4	**Benzaldehyde**		**Cinnamic acid**		**HCALD**		**COL**		**HCOL**	
loading (mg)	%select	%yield	%select	%yield	%select	%yield	%select	%yield	%select	%yield
150	62.0	20.3	36.0	11.8	0.3	0.1	1.7	0.5	0.3	0.1
300	52.2	20.5	38.6	15.0	2.1	0.8	4.6	1.8	2.4	1.0
900	55.9	15.8	41.6	11.6	0.4	0.1	2.0	0.6	0.0	0.0

4.6 Rate of FA Adding Effect

In this research, FA played an important role because it was not only acted as hydride donor but also as co-catalyst to protonate the starting cinnamaldehyde. Therefore, rate of adding FA was investigated. Figure 4.13a shows that the conversions of cinnamaldehyde were 34.1 and 36.7% at 10 μl per 2 min and 25 μl per 5 min FA adding rates, respectively. If FA (900 μL) was added at once at the beginning, the conversion was 40.2%. This results indicated that the increase of FA directly affected to the increase of the activity due to its co-catalyst ability (Yepez *et al.*, 2015). In terms of selectivity, the products of hydrogenation pathway were lower when FA was added too slow (10 μl per 2 min) or too fast (900 μl at once) (Figures 4.13b and 4.13c) . This is because FA rapidly decomposed on catalyst surface, turning to hydrogen gas, consequently leading to lack of hydride when all FA was added into the system at once and when too low FA was added to the system (10 μl per 2 min FA adding rate), giving a better selectivity to benzaldehyde formation.

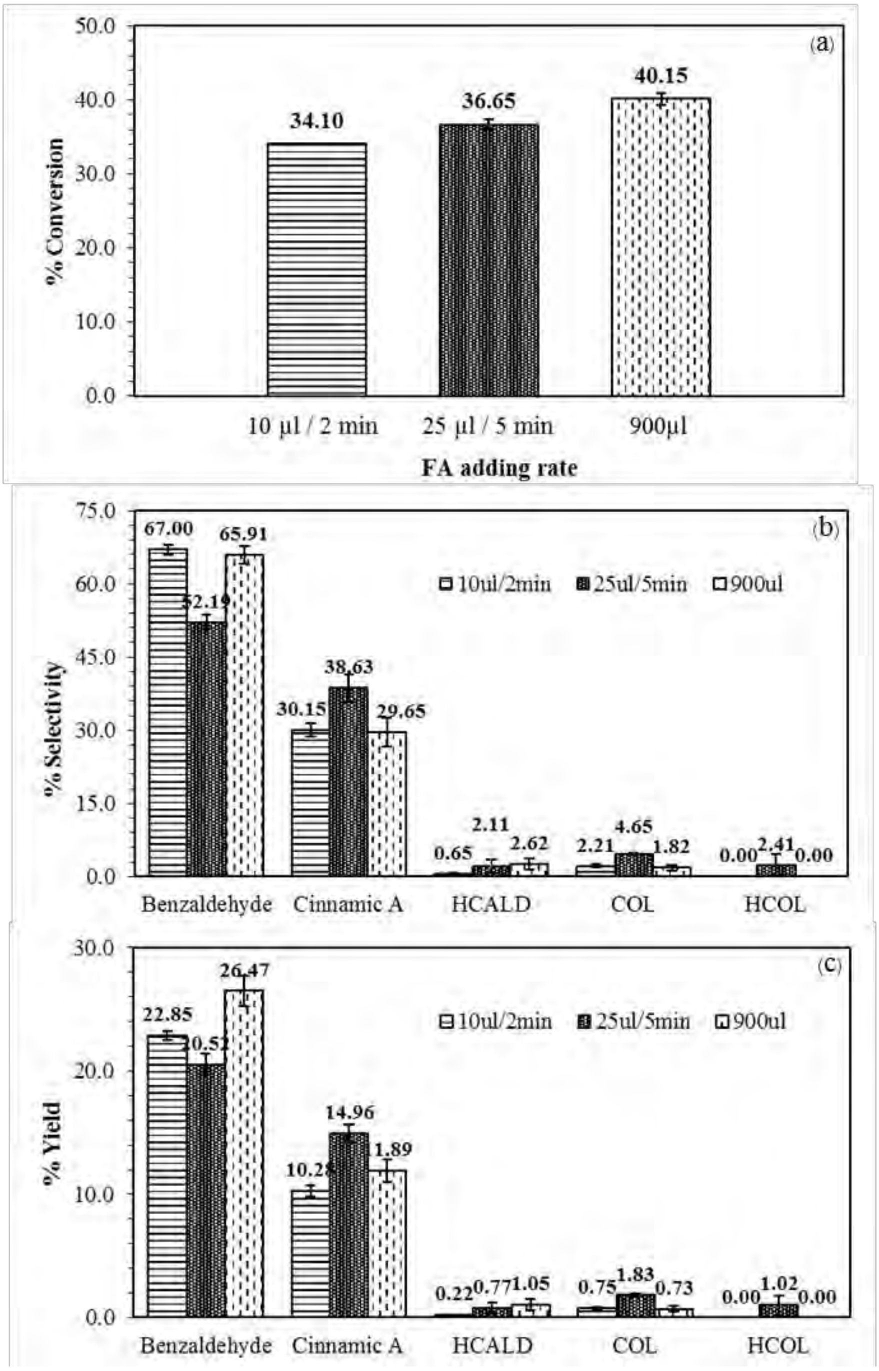

Figure 4.13 Plots of (a) overall conversion of CALD, and (b) selectivity and (c) yield of all products with various FA adding rate using 300 mg Ni_3Sn_4, 5 mmol CALD with THF at 60˚C and 3 h reaction time.

CHAPTER V
CONCLUSIONS AND RECOMMENDATIONS

5.1 Conclusions

Ni_3Sn, Ni_3Sn_2, and Ni_3Sn_4 intermetallics were successfully synthesized via mechanical alloying by using 43, 58, and 75% tin contents with nickel, respectively. The catalytic activity study revealed that Ni_3Sn_4 showed the highest activity and selectivity to hydrogenation pathway over other types of Ni_xSn_y intermetallics. Formic acid, hydrogen donor and co-catalyst, caused the hydrogenation reaction, leading to hydrocinnamaldehyde, cinnamyl alcohol, and hydrocinnamyl alcohol formation under mild conditions. Under the optimal conditions; 300 mg Ni_3Sn_4, 5 mmol CALD and 25 µl per 5 min of FA in 10 ml THF at 60˚C for 3 h reaction time, the maximum yield of COL was 1.83% with 36.65% conversion. Benzaldehyde and cinnamic acid were found as by-products via oxidation and retro-aldol condensation side reactions, respectively.

5.2 Recommendations

To study the Ni_xSn_y intermetallics efficiency in selective hydrogenation of α, β-unsaturated aldehyde reaction, other α, β-unsaturated aldehyde chemicals such as acrolein, citral, and acetophenone should be further studied. In addition, the reaction using hydrogen gas as hydrogen source with high pressure could be investigated to compare with using FA as hydrogen source under atmospheric pressure.

REFERENCES

Asedegbega, E.N., Bachiller, B.B., Guerrero, A.R., and Rodríguez, I.R. (2006) Modification of catalytic properties over carbon supported Ru–Cu and Ni–Cu bimetallics: I. Functional selectivities in citral and cinnamaldehyde hydrogenation. Applied Catalysis A: General, 300(2), 120-129.

Chen, H., Ji, H., Zhou, X., and Wang, L. (2010) Green synthesis of natural benzaldehyde from cinnamon oil catalyzed by hydroxypropyl-β-cyclodextrin. Tetrahedron, 66(52), 9888-9893.

Chen, X., Li, M., Guan, J., Wang, X., Williams, C.T., and Liang, C. (2012) Nickel–silicon intermetallics with enhanced selectivity in hydrogenation reactions of cinnamaldehyde and phenylacetylene. Industrial & Engineering Chemistry Research, 51(9), 3604-3611.

Delbecq, F. and Sautet, P. (1995) Competitive C=C and C=O adsorption of α-β-unsaturated aldehydes on Pt and Pd surfaces in relation with the selectivity of hydrogenation reactions: A theoretical approach. Journal of Catalysis, 152(2), 217–236.

Durndell, L.J., Parlett, C.M.A., Hondow, N.S., Isaacs, M.A., Wilson, K., and Lee, A.F. (2015) Selectivity control in Pt-catalyzed cinnamaldehyde hydrogenation. Scientific Reports, 5, 1-9.

Gallezot, P. and Richard, D. (1998) Selective hydrogenation of α, β-unsaturated aldehydes. Catalysis Reviews, 40(1-2), 81-126.

Gasteiger, H.A., Marković, N.M., and Ross, P.N. (1996) Structural effects in electrocatalysis: electrooxidation of carbon monoxide on Pt_3Sn single-crystal alloy surfaces. Catalysis Letters, 36(1), 1-8.

Guo, Z., Xiao, C., Maligal-Ganesh, R.V., Zhou, L., Goh, T.W., Li, X., Tesfagaber, D., Thiel, A., and Huang, W. (2014) Pt nanoclusters confined within metal–organic framework cavities for chemoselective cinnamaldehyde hydrogenation. ACS Catalysis, 4(5), 1340-1348.

Gutiérrez, V., Nador, F., Radivoy, G., and Volpe, M.A. (2013) Highly selective copper nanoparticles for the hydrogenation of α, β-unsaturated aldehydes in liquid phase. Applied Catalysis A: General, 464–465, 109-115.

Haan, J.L., Stafford, K.M., and Masel, R.I. (2010) Effects of the addition of antimony, tin, and lead to palladium catalyst formulations for the direct formic acid fuel cell. The Journal of Physical Chemistry C, 114(26), 11665-11672.

Hájek, J., Kumar, N., Mäki-Arvela, P., Salmi, T., Murzin, D.Y., Paseka, I., Heikkilä, T., Laine, E., Laukkanen, P., and Väyrynen, J. (2003) Ruthenium-modified MCM-41 mesoporous molecular sieve and Y zeolite catalysts for selective hydrogenation of cinnamaldehyde. Applied Catalysis A: General, 251(2), 385-396.

Hayden, B.E., Rendall, M.E., and South, O. (2003) Electro-oxidation of carbon monoxide on well-ordered Pt(111)/Sn surface alloys. Journal of the American Chemical Society, 125(25), 7738-7742.

Koo-amornpattana, W. and Winterbottom, J.M. (2001) Pt and Pt-alloy catalysts and their properties for the liquid-phase hydrogenation of cinnamaldehyde. Catalysis Today, 66(2–4), 277-287.

Li, C., Chen, Y., Zhang, S., Xu, S., Zhou, J., Wang, F., Wei, M., Evans, D.G., and Duan, X. (2013) Ni–In intermetallic nanocrystals as efficient catalysts toward unsaturated aldehydes hydrogenation. Chemistry of Materials, 25(19), 3888-3896.

Lin, W., Cheng, H., He, L., Yu, Y., and Zhao, F. (2013) High performance of Ir-promoted Ni/TiO_2 catalyst toward the selective hydrogenation of cinnamaldehyde. Journal of Catalysis, 303, 110-116.

Liu, H., Li, Z., and Li, Y. (2015) Chemoselective hydrogenation of cinnamaldehyde over a Pt-Lewis acid collaborative catalyst under ambient conditions. Industrial & Engineering Chemistry Research, 54(5), 1487-1497.

Liu, Z., Jackson, G.S., and Eichhorn, B.W. (2010) PtSn intermetallic, core–shell, and alloy nanoparticles as CO-tolerant electrocatalysts for H_2 oxidation. Angewandte Chemie International Edition, 49(18), 3173-3176.

Luo, Q., Feng, G., Beller, M., and Jiao, H. (2012) Formic acid dehydrogenation on Ni(111) and comparison with Pd(111) and Pt(111). The Journal of Physical Chemistry C, 116(6), 4149-4156.

Luo, Q., Wang, T., Beller, M., and Jiao, H. (2013) Hydrogen generation from formic acid decomposition on Ni(2 1 1), Pd(2 1 1) and Pt(2 1 1). Journal of Molecular Catalysis A: Chemical, 379, 169-177.

Mäki-Arvela, P., Hájek, J., Salmi, T., and Murzin, D.Y. (2005) Chemoselective hydrogenation of carbonyl compounds over heterogeneous catalysts. Applied Catalysis A: General, 292, 1-49.

Malobela, L.J., Heveling, J., Augustyn, W.G., and Cele, L.M. (2014) Nickel–cobalt on carbonaceous supports for the selective catalytic hydrogenation of cinnamaldehyde. Industrial & Engineering Chemistry Research, 53(36), 13910-13919.

Marteau, C., Ruyffelaere, F., Aubry, J.M., Penverne, C., Favier, D., and Nardello-Rataj, V. (2013) Oxidative degradation of fragrant aldehydes. Autoxidation by molecular oxygen. Tetrahedron, 69(10), 2268-2275.

Mertens, P.G.N., Cuypers, F., Vandezande, P., Ye, X., Verpoort, F., Vankelecom, I.F.J., and De Vos, D.E. (2007) Ag^0 and Co^0 nanocolloids as recyclable quasihomogeneous metal catalysts for the hydrogenation of α, β-unsaturated aldehydes to allylic alcohol fragrances. Applied Catalysis A: General, 325(1), 130-139.

Mertens, P.G.N., Vandezande, P., Ye, X., Poelman, H., Vankelecom, I.F.J., and De Vos, D.E. (2009) Recyclable Au^0, Ag^0 and Au^0–Ag^0 nanocolloids for the chemoselective hydrogenation of α, β-unsaturated aldehydes and ketones to allylic alcohols. Applied Catalysis A: General, 355(1–2), 176-183.

Morakotjinda, M., Fakpan, K., Yotkaew, T., Tosangthum, N., Krataithong, R., Daraphan, A., Siriphol, P., Wila, P., Vetayanugul, B., and Tongsri, R. (2010) Gas atomization of low melting-point metal powders. Chiang Mai Journal of Science, 37(1), 55-63.

Pham-Huu, C., Keller, N., Ehret, G., Charbonniere, L.J., Ziessel, R., and Ledoux, M.J. (2001) Carbon nanofiber supported palladium catalyst for liquid-phase reactions: An active and selective catalyst for hydrogenation of cinnamaldehyde into hydrocinnamaldehyde. Journal of Molecular Catalysis A: Chemical, 170(1–2), 155-163.

Pithakratanayothin, S., Ruangdaj, T., Chaisuwan, T., and Wongkasemjit, S. Influences of M-Sn intermetallics (M=Ni,Cu) prepared by mechanical alloying on phenol hydroxylation Catalysis Science & Technology. (To be submitted).

Prakash, M.G., Mahalakshmy, R., Krishnamurthy, K.R., and Viswanathan, B. (2016) Studies on Ni–M (M = Cu, Ag, Au) bimetallic catalysts for selective hydrogenation of cinnamaldehyde. Catalysis Today, 263, 105-111.

Rautio, A.R., Mäki-Arvela, P., Aho, A., Eränen, K., and Kordas, K. (2015) Chemoselective hydrogenation of citral by Pt and Pt-Sn catalysts supported on TiO_2 nanoparticles and nanowires. Catalysis Today, 241, 170-178.

Ramos de Debiaggi, S., Deluque Toro, C., Cabeza, G.F., and Fernández, A.G. (2013) Ab initio study of the cohesive properties, electronic structure and thermodynamic stability of the Ni–In and Ni–Sn intermetallics. Journal of Alloys and Compounds, 576, 302-316.

Rodiansono, Khairi, S., Hara, T., Ichikuni, N., and Shimazu, S. (2012) Highly efficient and selective hydrogenation of unsaturated carbonyl compounds using Ni-Sn alloy catalysts. Catalysis Science & Technology, 2(10), 2139-2145.

Santori, G.F., Casella, M.L., and Ferretti, O.A. (2002) Hydrogenation of carbonyl compounds using tin-modified platinum-based catalysts prepared via surface organometallic chemistry on metals (SOMC/M). Journal of Molecular Catalysis A: Chemical, 186(1–2), 223-239.

Shirai, M., Tanaka, T., and Arai, M. (2001) Selective hydrogenation of α, β-unsaturated aldehyde to unsaturated alcohol with supported platinum catalysts at high pressures of hydrogen. Journal of Molecular Catalysis A: Chemical, 168(1–2), 99-103.

Singh, A.K., Singh, S., and Kumar, A. (2016) Hydrogen energy future with formic acid: a renewable chemical hydrogen storage system. Catalysis Science & Technology, 6(1), 12-40.

Stevanović, S., Tripković, D., Tripković, V., Minić, D., Gavrilović, A., Tripković, A., and Jovanović, V.M. (2014) Insight into the effect of Sn on CO and formic acid oxidation at PtSn catalysts. The Journal of Physical Chemistry C, 118(1), 278-289.

Swift, H.E., and Bozik, J.E. (1968) Metallic phases and activities of nickel-tin-silica catalysts. Journal of Catalysis, 12(1), 5-14.

Taniya, K., Jinno, H., Kishida, M., Ichihashi, Y., and Nishiyama, S. (2012) Preparation of Sn-modified silica-coated Pt catalysts: A new PtSn bimetallic model catalyst for selective hydrogenation of crotonaldehyde. Journal of Catalysis, 288, 84-91.

Wang, D., Jiang, H., Zong, X., Xu, Q., Ma, Y., Li, G., and Li, C. (2011) Crystal facet dependence of water oxidation on $BiVO_4$ sheets under visible light irradiation. Chemistry – A European Journal, 17(4), 1275-1282.

Wang, K., Gasteiger, H.A., Markovic, N.M., and Ross, P.N. (1996) On the reaction pathway for methanol and carbon monoxide electrooxidation on Pt-Sn alloy versus Pt-Ru alloy surfaces. Electrochimica Acta, 41(16), 2587-2593.

Wei, Z., Sun, J., Li, Y., Datye, A.K., and Wang, Y. (2012) Bimetallic catalysts for hydrogen generation. Chemical Society Reviews, 41(24), 7994-8008.

Wienhöfer, G., Westerhaus, F.A., Junge, K., and Beller, M. (2013) Fast and selective iron-catalyzed transfer hydrogenations of aldehydes. Journal of Organometallic Chemistry, 744, 156-159.

Yadav, G.D., and Fernandes, G.P. (2013) Selective synthesis of natural benzaldehyde by hydrolysis of cinnamaldehyde using novel hydrotalcite catalyst. Catalysis Today, 207, 162-169.

Yadav, M., and Xu, Q. (2012) Liquid-phase chemical hydrogen storage materials. Energy & Environmental Science, 5(12), 9698-9725.

Yepez, A., Hidalgo, J.M., Pineda, A., Cerny, R., Jisa, P., Garcia, A., Romero, A.A., and Luque, R. (2015) Mechanistic insights into the hydroconversion of cinnamaldehyde using mechanochemically-synthesized Pd/Al-SBA-15 catalysts. Green Chemistry, 17(1), 565-572.

Yoo, J.S., Abild-Pedersen, F., Nørskov, J.K., and Studt, F. (2014) Theoretical analysis of transition-metal catalysts for formic acid decomposition. ACS Catalysis, 4(4), 1226-1233.

Zhang, L., Winterbottom, J.M., Boyes, A.P., and Raymahasay, S. (1998) Studies on the hydrogenation of cinnamaldehyde over Pd/C catalysts. Journal of Chemical Technology & Biotechnology, 72(3), 264-272.

Zhao, J., Xu, X., Li, X., and Wang, J. (2014) Promotion of Sn on the Pd/AC catalyst for the selective hydrogenation of cinnamaldehyde. Catalysis Communications, 43, 102-106.

CURRICULUM VITAE

Name: Ms. Anchernsiri Noomnual

Date of Birth: January 23, 1992

Nationality: Thai

University Education:

2011–2014 Bachelor Degree of Chemistry, Faculty of Science, Kasetsart University, Bangkok, Thailand

Proceedings:

1. Noomnual, A., Pithakratanayothin, S., Chaisuwan, T., and Wongkasemjit, S. (2017, May 15-17) Type of chemical reaction from cinnamaldehyde using nickel-tin intermetallics under mild conditions. The TechConnect World Innovation Conference, Washington D.C., USA.
2. Noomnual, A., Pithakratanayothin, S., Chaisuwan, T., and Wongkasemjit, S. (2017, May 23) Catalytic activity of Ni_xSn_y intermetallics. Proceedings of the 9th Research Symposium on Petrochemical and Materials Technology; and 23th PPC Symposium on Petroleum, Petrochemicals, and Polymers, Bangkok, Thailand.